

Influence of carbon-ion irradiation on the superconducting critical properties of MgB₂ thin films

Soon-Gil Jung^{1,2}, Seung-Ku Son^{1,2}, Duong Pham², Weon Cheol Lim³, Jonghan Song³, Won Nam Kang², and Tuson Park^{1,2}

¹Center for Quantum Materials and Superconductivity (CQMS), Sungkyunkwan University,
Suwon 16419, Republic of Korea

²Department of Physics, Sungkyunkwan University, Suwon 16419, Republic of Korea

³Advanced Analysis Center, Korea Institute of Science and Technology (KIST),
Hwarang-ro 14-gil 5, Seongbuk-gu, Seoul 02792, Republic of Korea

E-mail: wnkang@skku.edu and tp8701@skku.edu

Fax: +82 31 290 7056

Abstract

We investigate the influence of carbon-ion irradiation on the superconducting critical properties of MgB₂ thin films. MgB₂ films of two thicknesses viz. 400 nm (MB400nm) and 800 nm (MB800nm) were irradiated by 350 keV C ions having a wide range of fluence, $1 \times 10^{13} - 1 \times 10^{15}$ C atoms/cm². The mean projected range (R_p) of 350 keV C ions in MgB₂ is 560 nm, thus the energetic C ions will pass through the MB400nm, whereas the ions will remain into the MB800nm. The superconducting transition temperature

(T_c), upper critical field (H_{c2}), c -axis lattice parameter, and corrected residual resistivity (ρ_{corr}) of both the films showed similar trends with the variation of fluence. However, a disparate behavior in the superconducting phase transition was observed in the MB800nm when the fluence was larger than 1×10^{14} C atoms/cm² because of the different T_c s between the irradiated and non-irradiated parts of the film. Interestingly, the superconducting critical properties, such as T_c , H_{c2} , and J_c , of the irradiated MgB₂ films, as well as the lattice parameter, were almost restored to those in the pristine state after a thermal annealing procedure. These results demonstrate that the atomic lattice distortion induced by C-ion irradiation is the main reason for the change in the superconducting properties of MgB₂ films.

PACS numbers: 74.25.Op, 74.25.Sv, 74.62.En, 74.70.Ad

keywords: carbon-ion irradiation, upper critical field, thermal annealing, MgB₂ thin films

1. Introduction

Magnesium diboride (MgB_2) has promising superconducting (SC) properties for technological applications, such as a high transition temperature (T_c) of ~ 40 K [1], high upper critical field (H_{c2}) [2,3], and large critical current density (J_c) [4,5]. In addition, two clear SC gaps of Δ_σ and Δ_π in MgB_2 have stimulated studies to understand the mechanism of its superconductivity [2,6,7]. Carbon (C) substitution for boron (B), $\text{MgB}_{2-x}\text{C}_x$, is well known as one of the most effective methods to improve H_{c2} and J_c despite a reduction in T_c caused by a suppression of the large SC gap Δ_σ . The C substitution considerably affects the σ -bonding derived from the in-plane p_{xy} B orbitals, whereas it hardly changes the π -bonding related to the out-of-plane p_z B orbitals [2,8-11].

Neutron irradiation in MgB_2 also has a significant influence on the B sites because of the thermal neutron capture reaction. The ^{10}B atoms ($\sim 20\%$ in natural B) that capture the thermal neutrons decay into an alpha (α) particle and a ^7Li nucleus, leading to homogeneous disorders in MgB_2 and an improvement in both H_{c2} and J_c [2,12-15]. In addition, light particles, such as protons and α particles, have often been reported to be effective sources of irradiation to enhance H_{c2} and J_c of MgB_2 [16,17]. On the other hand, heavy-ion irradiations are less effective in improving J_c of MgB_2 [18,19]. In general, high energy heavy-ion irradiations into SC materials produce columnar defects along the ion tracks, which act as a strong flux-pinning source to improve the in-field J_c of the high- T_c cuprate superconductors [20,21]. However, heavy-ion irradiations in MgB_2 seem to rapidly suppress its superconductivity rather than improve its critical SC parameters, such as H_{c2} and J_c [18,22]. For these reasons, irradiation

studies of MgB₂ have been mostly focused on neutron irradiation.

Irradiation is a unique technique that makes it possible to examine the effects of radiation and additional defects in an identical sample [13,23,24]. The study of radiation effects on a superconductor is important to test their application in a radiation environment, such as space, fusion reactions, and so on [13,23]. In addition, ion irradiations can create defects in target materials mainly by nuclear stopping of energetic ions, although the exact mechanism for the formation of defects is still debatable [23,25]. In superconductors, defects are normally beneficial for the enhancement of SC critical properties, especially in-field J_c , because defects in type-II superconductors can interrupt vortex motion. Therefore, understanding the effects of defects on SC critical properties is a key issue for technological applications of superconductors as well as for scientific advancement [26,27].

In this study, we report the influence of carbon-ion irradiation on the superconducting critical properties of *c*-axis-oriented MgB₂ thin films with thicknesses of 400 and 800 nm. The C was selected as the irradiating ion source because C has been known as one of the most effective elements to enhance H_{c2} and in-field J_c of MgB₂. Carbon ions of various fluences ranging between 1×10^{13} and 1×10^{15} C atoms/cm² with an incident energy of 350 keV (mean projected range R_p : \sim 560 nm) were irradiated into the prepared MgB₂ films. The superconducting properties after irradiations were slightly different depending on whether the irradiated C ions penetrated fully the film (400 nm) or were implanted into the film (800 nm). However, the degraded superconductivity of both the irradiated MgB₂ films was almost recovered to those in the pristine state after a thermal annealing procedure. These results indicate that the effect of the implanted C ions on the superconductivity of MgB₂ films is

insignificant, whereas the displacement damage by irradiation is crucial to the change in T_c , H_{c2} , and J_c of MgB₂.

2. Experimental

High-quality MgB₂ thin films of thicknesses 400 nm (MB400nm) and 800 nm (MB800nm) were fabricated on *c*-cut Al₂O₃ substrates for C-ion irradiation studies by using a hybrid physical-chemical vapor deposition (HPCVD) method, the details of the growth technique described earlier [28,29]. C-ion irradiation was carried out using Cockcroft-Walton type 400 kV ion beam accelerator at Korea Institute of Science and Technology (KIST), Seoul. Various fluences of 1×10^{13} (1E13), 5×10^{13} (5E13), 1×10^{14} (1E14), 2×10^{14} (2E14), 5×10^{14} (5E14), and 1×10^{15} (1E15) C atoms/cm² with a tilted angle of 7° to avoid channeling effects during irradiations were irradiated into the prepared MgB₂ films at room temperature. The mean projected range (R_p) of the irradiated C ions, with an incident beam energy of 350 keV, was estimated to be around 560 nm from SRIM (The Stopping and Range of Ions in Matter), a Monte Carlo simulation program [30]. Therefore, the irradiated C ions were remained into the MB800nm due to the R_p being greater than the film thickness whereas most of the ions penetrated through the MB400nm.

The thickness of the MgB₂ thin films was measured by using a scanning electron microscope (SEM), and the crystallinity of the films before and after irradiation was checked by using an x-ray diffractometer (XRD). The electrical resistivity (ρ) was measured by using the standard 4-probe technique with gold (Au) coating on the 4-point contact regions to achieve good ohmic contact. The upper critical field (H_{c2}) for a magnetic field applied perpendicular to the *ab* plane

of the surface of the film was measured by the Physical Property Measurement System (PPMS 9 T, Quantum Design) and the temperature dependence of magnetization, $M(T)$, was measured by using the Magnetic Property Measurement System (MPMS 5 T, Quantum Design) before and after C-ion irradiation.

Thermal annealing was carried out for the MB400nm and MB800nm irradiated with the highest fluence of 1×10^{15} atoms/cm² (1E15). In addition, a non-irradiated MB400nm was also prepared for the thermal annealing to check only annealing effect on the pristine sample. Three films were wrapped in tantalum (Ta) foil to minimize the Mg decomposition during thermal annealing, sealed inside an evacuated quartz tube, and then the ampoules were annealed at temperatures of 200, 300, 400, and 500 °C for 30 min. in a box furnace. The same irradiated films with the 1E15 were consecutively annealed at each temperature, and the non-irradiated MB400nm was annealed only at 500 °C. The annealing experiments were conducted at temperatures up to 500 °C as large Mg deficiency can be induced at higher temperatures [31]. $M(T)$ and x-ray diffraction patterns of the irradiated films were examined after the annealing procedure for each annealing temperature (T_A). In addition, ρ , H_{c2} , and magnetization hysteresis ($M - H$) loops for the films annealed at $T_A = 500$ °C were investigated by using the same techniques mentioned above.

3. Results and discussion

Figure 1 describes the mean projected range (R_p) of the irradiated C ions with a beam energy of 350 keV into MgB₂, simulated by using SRIM (Stopping and Range of Ions in Matter) software [30], presenting that most of the C ions are stopped at around $R_p \sim 560$ nm after

undergoing a series of collisions with the Mg and B atoms. In view of the magnitude of the R_p , two MgB₂ thin films having thicknesses of 400 nm (MB400nm) and 800 nm (MB800nm) were irradiated with the 350 keV C ions, and while most of the energetic C ions penetrated through MB400nm, as shown in figure 1, they remained in MB800nm as defects or were substituted into B sites.

Figures 2(a) and (b) show the temperature dependence of the normalized electrical resistivity, $\rho(T)/\rho(41\text{ K})$, near the superconducting (SC) transition regions for pristine (pri.) and irradiated MgB₂ films of MB400nm and MB800nm, respectively, whereby C-ion irradiation into MgB₂ thin films resulted in suppression of the SC transition temperature (T_c). In this case, T_c was determined from 50% of the normal state resistivity value at SC onset temperature, as indicated by arrows in figures 2(a) and (b). For the films irradiated with higher fluences than 1×10^{14} atoms/cm² (1E14), the SC transition width of MB800nm is much broader than that of MB400nm, while T_c of MB800nm is higher than that of MB400nm. As shown in figures 2(c) and (d), the zero-field-cooled (ZFC) and field-cooled (FC) dc magnetization (M) data for MB400nm and MB800nm also showed similar results to the electrical resistivity. Here, $M(T)$ values were normalized by the absolute ZFC M value at 5 K for comparison. The onset temperature for the diamagnetic signal gradually reduces with increasing fluence for both MB400nm and MB800nm. A kink in the ZFC $M(T)$ data, however, is apparent in the SC transition region for MB800nm irradiated with large fluences of 5×10^{14} (5E14) and 1×10^{15} atoms/cm² (1E15), while it is absent for MB400nm. Since the thickness of MB800nm is larger than R_p (~ 560 nm), the kink observed in the MB800nm may be ascribed to two different T_c s between the irradiated and non-irradiated parts of the MgB₂ films.

The temperature dependence of electrical resistivity (ρ) is comparatively plotted in figures 3(a) and (b) for MB400nm and MB800nm before and after irradiation, respectively. The resistivity increases over the whole temperature range with increasing fluence of the C-ion radiation. Figures 3(c) and (d) present a plot of T_c as a function of the residual resistivity, $\rho_{41K} = \rho(41\text{ K})$, and corrected residual resistivity (ρ_{corr}) for MB400nm and MB800nm, respectively, where ρ_{corr} was introduced to exclude the effects of grain boundaries on the resistivity and is defined as $\rho_{\text{corr}} = \rho_{41K} \times \Delta\rho_{\text{ideal}}/\Delta\rho$, where $\Delta\rho = \rho(300\text{ K}) - \rho(41\text{ K})$ and $\Delta\rho_{\text{ideal}}$ is $\Delta\rho$ of MgB_2 with full connectivity [12,15,32]. Here, we used $\Delta\rho_{\text{ideal}} = 4.3\ \mu\Omega\cdot\text{cm}$ determined from a MgB_2 single crystal because $\Delta\rho$ of the pristine MB400nm and MB800nm is $6.4\ \mu\Omega\cdot\text{cm}$ and $5.9\ \mu\Omega\cdot\text{cm}$, respectively [32]. For fluences higher than $1\text{E}14$, the ρ_{41K} values of MB800nm is much larger than those of MB400nm, while the reduction rate of T_c for MB800nm is weaker than that for MB400nm. When ρ_{41K} is converted to ρ_{corr} , however, T_c s of MB400nm and MB800nm are well scaled on a single curve, as shown in figure 3(d) [13,15]. These results indicate that, despite a larger residual resistivity than MB400nm, the higher T_c in MB800nm results from the proximity effect between the irradiated and non-irradiated parts in it. In addition, the decrease in T_c of both the films can be attributed to enhanced intra-grain scattering by C-ion irradiation [13,32], whereas the effect of implanted C ions on T_c seems negligible in the MB800nm films.

Figures 4(a) and (b) show the x-ray diffraction (XRD) patterns of a $\theta - 2\theta$ scan for pristine and irradiated MB400nm and MB800nm, respectively, showing a shift of (00 l) peak positions of MgB_2 due to C-ion irradiation. Figures 4(c) and (d) are the magnified views of the (002) peak of MB400nm and MB800nm, respectively. With increasing fluence, the peak position is progressively shifted towards a lower angle and the peak width is broadened [12,14,15,33],

reflecting an expansion of the c -axis lattice parameter and degradation of crystallinity of the MgB_2 films. The (002) peak is considerably broadened for the irradiated MB800nm than for the MB400nm. In addition, MB800nm irradiated with $1\text{E}15$ show a double-peak like behavior due to the implanted C ions around the R_p , as shown in figure 1.

The dependence on C-ion fluence of the c -axis lattice constant, $\rho_{41\text{K}}$, and T_c for MB400nm and MB800nm are plotted in figures 5(a), (b), and (c), respectively. In comparison with the pristine films, the c -axis lattice parameter of MB400nm and MB800nm irradiated with $1\text{E}15$ fluence is increased by 0.75% and 1.22%, respectively. The expanded lattice parameter in irradiated films underlines the fact that displacement damage by nuclear stopping (elastic scattering between energetic C ions and Mg/B atoms) is more prominent than the damage by electronic stopping (interaction between the energetic C ions and electrons of MgB_2) for an increase of $\rho_{41\text{K}}$ and suppression of T_c [23]. A sudden increase in $\rho_{41\text{K}}$ of MB800nm at 2×10^{14} atoms/cm² ($2\text{E}14$) implies that the implanted C ions create substantial defects due to large damage events around R_p , while the T_c suppression is smeared out due to the proximity effects between the irradiated and non-irradiated parts of the MgB_2 films.

In order to study the effect of C-ion irradiation on the upper critical field (H_{c2}) of MB400nm and MB800nm, the electrical resistivity was measured as a function of temperature for magnetic fields applied perpendicular to the ab plane. Figures 6(a) and (b) display the $\rho(T)$ curves in a magnetic field for the pristine and C-ion irradiated MB400nm with $2\text{E}14$ fluence, respectively. It will be shown that $2\text{E}14$ is an optimal fluence for the enhancement of H_{c2} in this study. Here, $\rho(T)$ is normalized by the normal state resistivity (ρ_n) at each magnetic field for comparison, and H_{c2} is determined as the middle point of the SC transition, as indicated by arrows in figures 6(a)

and (b). H_{c2} s of MB400nm and MB800nm plotted as a function of temperature for various fluences are shown in figures 6(c) and 6 (d), respectively, where all $H_{c2}(T)$ curves are well explained by the two-band Ginzburg-Landua (GL) theory [34]. The solid lines in figures 6(c) and (d) are representative fitting curves for $H_{c2}(T)$ of the pristine and MgB₂ films irradiated with a fluence of 2E14.

The upper critical field at zero Kelvin, $H_{c2}(0)$, estimated from the data in figures 6(c) and (d) is plotted as a function of fluence and T_c in figures 7(a) and (b), respectively. $H_{c2}(0)$ of the pristine MB400nm and MB800nm is 6.16 and 5.85 T, respectively, which increases rapidly with increasing fluence and reaches a maximum of 11.09 T for MB400nm and 9.78 T for MB800nm at 2E14, and decreases slowly with further increasing fluence. Both the films show the largest enhancement of $H_{c2}(0)$ at the same fluence of 2E14. Even though there occurs a large improvement in $H_{c2}(0)$ by C-ion irradiation, the T_c suppression in MgB₂ films by C-ion irradiation, as shown in figure 7(b), is relatively small and comparable with the results of irradiation of MgB₂ by other particles, such as neutrons, α particles, oxygen ions, and so on [12,15,17,33]. In addition, the T_c of MB800nm is insensitive to the irradiation compared to that of MB400nm, suggesting that undamaged SC layer is helpful to improve SC critical properties, such as H_{c2} and critical current density (J_c), while minimizing T_c reduction.

Figure 8 shows the evolution of XRD patterns around the (002) peak for the pristine and C-ion irradiated MB400nm and MB800nm with the fluence of 1E15, when the irradiated films were subsequently annealed for 30 min. at $T_A = 200, 300, 400,$ and 500 °C. The (002) peak position of the irradiated film, which is shifted towards a lower angle than that for the pristine film, moves to a higher angle with increasing annealing temperature and is close to that of the

pristine film for $T_A = 500$ °C. Figure 9 shows a plot of the c -axis lattice parameter of the irradiated MgB₂ films as a function of the annealing temperature. Unlike MB400nm, the c -axis lattice parameter of MB800nm does not fully regain its value to that in the pristine state after thermal annealing at 500 °C, indicating that the C ions implanted into MB800nm remain in the films as interstitial defects. These results indicate that lattice distortion by Frenkel disorder, such as interstitials and vacancies, is mainly produced by C ions traveling through the MgB₂ because thermal annealing for a short period (30 min.) was sufficient enough to restore the expanded lattice parameter of the irradiated MgB₂ films to that in the pristine state [13,35,36].

Figures 10(a) and (b) show the temperature dependence of ZFC and FC dc magnetization (M) for the annealed MB400nm and MB800nm films, respectively. The SC regions of both the films degraded by irradiation are gradually recovered as the annealing temperature (T_A) increases. Furthermore, the kink observed in MB800nm irradiated with a fluence of 1E15 disappears by thermal annealing, underlining that it originated due to the T_c difference between the irradiated and non-irradiated layers in MB800nm, as discussed in figure 2(d). It was noted that the magnetization of MB400nm did not fully recover to that of the pristine state after annealing at 500 °C, even though its c -axis lattice parameter was completely restored, as shown in figures 8(a) and 9. The ZFC transition of the pristine MB400nm become slightly broad after annealed at 500 °C, probably due to a decomposition of Mg during the thermal annealing [31], which would be one of the reasons why the T_c of irradiated films does not recover completely after thermal annealing.

The SC transition temperature (T_c) and upper critical field (H_{c2}) of the irradiated films (1E15), after annealing them at $T_A = 500$ °C, were determined from electrical resistivity measurements

and compared for various fluences of C-ion irradiation. The results were similar to the $M-T$ results presented in figure 10, and the T_c of the annealed films is slightly lower than that of the pure films, as shown in figure 11(a). T_c s of the annealed films decrease linearly with the corrected residual resistivity (ρ_{corr}) which is relatively larger for the annealed films than the pristine films, and may be ascribed to amorphization in some regions or Mg decomposition during the thermal annealing procedure [31]. The fact that $H_{c2}(0)$ of the annealed films is slightly higher than that of the pristine samples, as presented in figure 11(b), may be due to the same reason as in the case of ρ_{corr} . The fluence of 1E15 corresponds to a concentration of $\sim 8 \times 10^{19}$ C atoms/cm³ at R_p , which is much lower than the concentration of MgB₂, which is $\sim 1.15 \times 10^{22}$ Mg atoms/cm³ and $\sim 2.29 \times 10^{22}$ B atoms/cm³ [37,38]. This relatively small fraction of C ions may be one of the possible reasons for the negligible effects of the implanted C ions as impurities in the annealed MB800nm. More detailed studies, such as multiple injections and microscopic investigation, will be needed to make a definitive conclusion on the role of implanted C ions.

Figure 12 shows the magnetic field dependence of critical current density (J_c) at 5 K for MB400nm and MB800nm: pristine (squares), 1E15 (circles), and annealed at 500 °C (triangles). The J_c was estimated from the magnetization hysteresis ($M-H$) loops by using Bean's critical state model ($J_c = 30\Delta M/r$) [5], where ΔM is the height of the $M-H$ loops and r is the corresponding radius of the total area of the film's surface, and the $M-H$ loops were measured in magnetic fields applied perpendicular to the film's plane. A large self-field J_c of pristine films and its rapid drop in magnetic fields indicate a high quality of MB400nm and MB800nm. The field performance of J_c for both the irradiated films is much stronger than that in the pristine

state because of additional pinning sites created by C-ion irradiation, whereas a significant reduction of the J_c at zero field is due to the suppression of superconducting regions and T_c reduction. The J_c value of irradiated MB800nm is slightly larger than that of irradiated MB400nm because of the presence of a non-irradiated layer in MB800nm films. Surprisingly, the field performance of J_c for both the irradiated films almost recovered to that of the pristine state after thermal annealing at $T_A = 500$ °C, which is in sharp contrast to the thermal annealing effects on $J_c(H)$ for neutron-irradiated MgB₂ polycrystals [14]. A similar field performance of J_c between the annealed MB400nm and MB800nm is consistent with the results on the $H_{c2}(0)$ described in figure 11.

In neutron-irradiated MgB₂, SC properties, such as T_c , the c -axis lattice constant, and $H_{c2}(0)$, are close to the values in the pristine state after annealing at 500 °C, whereas the field performance of J_c is stronger than that of the pristine state. Since J_c , the depinning critical current density, is largely influenced by non-SC regions, such as defects, the thermal annealing effects on $J_c(H)$ for neutron-irradiated MgB₂ implies that thermodynamically irreversible defects are formed in MgB₂ by neutron irradiation [14,39,40]. Considering that the effects of irradiation and thermal neutron capture reactions are complex, however, it is difficult to understand the exact nature of the defects produced by neutron irradiation. On the other hand, the modified SC properties of high-quality MgB₂ thin films, such as T_c , H_{c2} , and the c -axis lattice constant, as well as the enhanced J_c by C-ion irradiation were almost fully reversed to the values in the pristine state after thermal annealing for a short period of time. These results indicate that the degraded superconductivity of MgB₂ by C-ion irradiations is mainly associated with the atomic lattice distortion caused by displacement damage, which is a reversible deformation, and the

recovery of the SC characteristics to the pristine state by thermal annealing could be ascribed to the recovery of its crystallinity.

4. Conclusions

In conclusion, we studied the effects of carbon-ion irradiation on the superconducting critical properties of two MgB₂ thin films with different thicknesses: 400 nm and 800 nm. One film was thinner than the mean projected range ($R_p \sim 560$ nm) of irradiated C ions and the other was thicker than R_p . The superconducting transition temperatures (T_c) of both the films gradually decreased with increasing fluence of the C ions, and were accompanied by an expansion of the c -axis lattice constant. In addition, the residual resistivity (ρ_{41K}) and upper critical field (H_{c2}) considerably increased after C-ion irradiation because of the defects produced by the irradiation. On the other hand, the effect of the implanted C ions on H_{c2} was not prominent compared to other irradiation effects due to the strong interaction between the irradiated and non-irradiated layers in MgB₂ films. Interestingly, the degraded superconductivity and expanded lattice parameter of the irradiated MgB₂ were almost regained to that in the pristine state after thermal annealing at 500 °C for 30 min. In particular, the improved field performance of the critical current density (J_c) by C-ion irradiation was also restored to that in the pristine state, underpinning the fact that the lattice distortion induced by the irradiation is the main origin of the modified superconducting properties of irradiated MgB₂ films.

Acknowledgements

This work was supported by the National Research Foundation (NRF) of Korea by a grant funded by the Korean Ministry of Science, ICT and Planning (No. 2012R1A3A2048816) and the Basic Science Research Program through the National Research Foundation of Korea (NRF) funded by the Ministry of Education (NRF-2016R1D1A1B03934513 and NRF-2015R1D1A1A01060382). This work is also supported by KIST institutional program (2V06030).

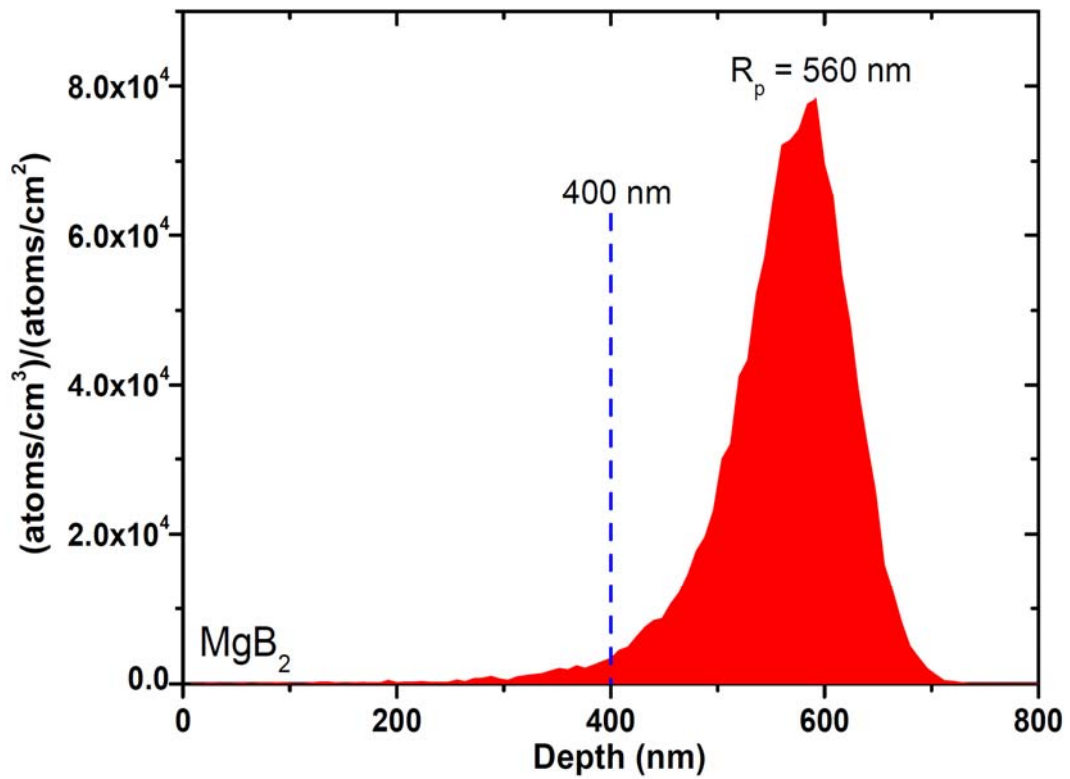


Figure 1. SRIM simulation for the range of irradiated carbon (C) ions with incident energy of 350 keV in MgB₂, where the density of MgB₂ is 2.57 g/cm³ and the estimated mean projected range (R_p) is around 560 nm. Most of the irradiated C ions pass through MB400nm, but for the MB800nm, the ions are distributed around 560 nm below the MgB₂ surface.

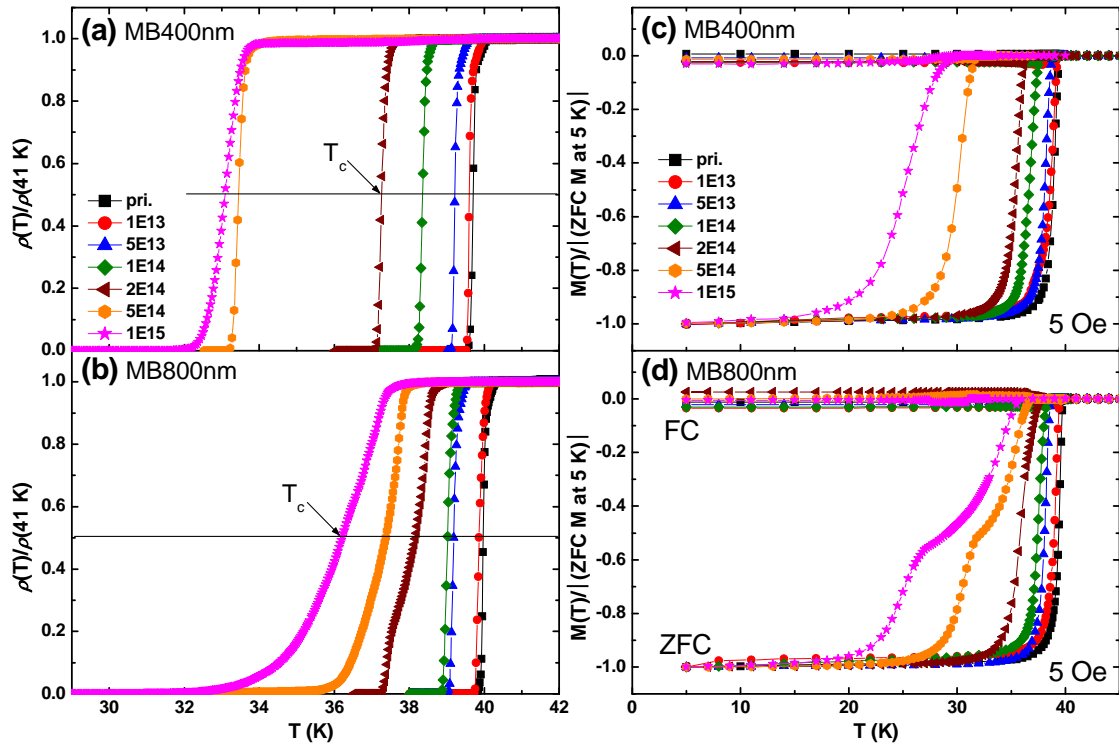


Figure 2. Superconducting transitions measured by [(a) and (b)] electrical resistivity (ρ) and [(c) and (d)] magnetization (M) for MB400nm and MB800nm at different damage levels of irradiation. Kinks in the $M(T)$ of MB800nm result from a different T_c between the irradiated and non-irradiated layers of MgB_2 .

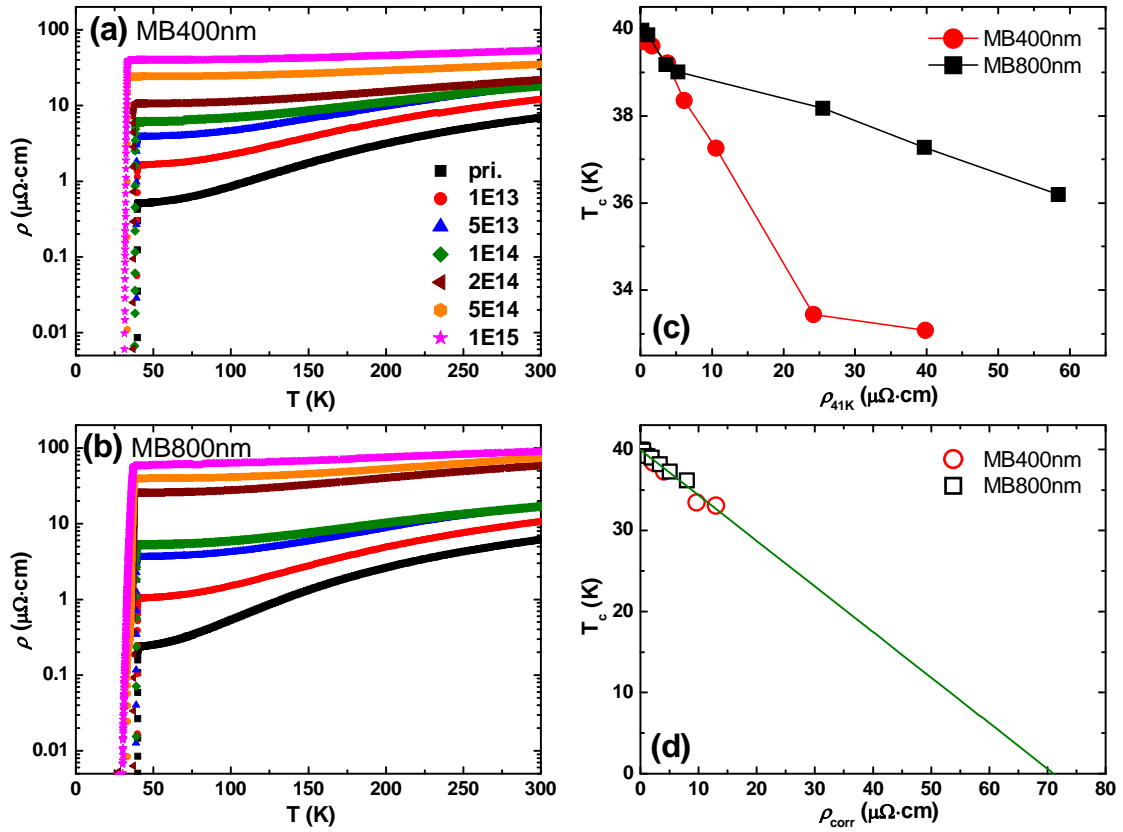


Figure 3. (a) and (b) Temperature dependence of resistivity (ρ) of MB400nm and MB800nm, respectively. (c) and (d) Superconducting transition temperature (T_c) of MB400nm and MB800nm as functions of residual resistivity at 41 K ($\rho_{41\text{K}}$) and corrected residual resistivity (ρ_{corr}), respectively. T_c is determined from the 50% resistivity drop from the residual resistivity, as shown in figures 2(a) and (b). The T_c variations in irradiation are well expressed by one curve using ρ_{corr} .

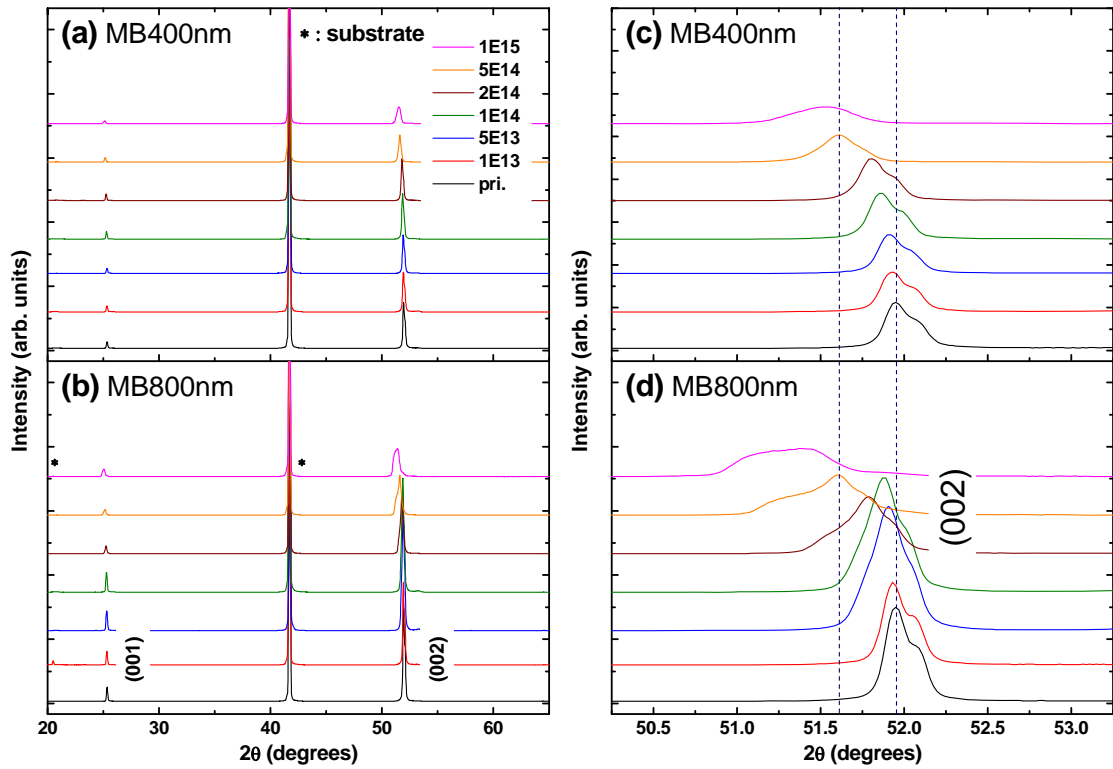


Figure 4. (a) and (b) X-ray diffraction (XRD) patterns of MB400nm and MB800nm, respectively, with various fluences. (c) and (d) Enlarged view near (002) peak for MB400nm and MB800nm, respectively. The shift in the peak position increases with increasing fluence, and the (002) peak of MB800nm becomes much broader at large fluences compared to that of MB400nm due to the implanted C ions inside the film. Dashed lines are guides for the eyes.

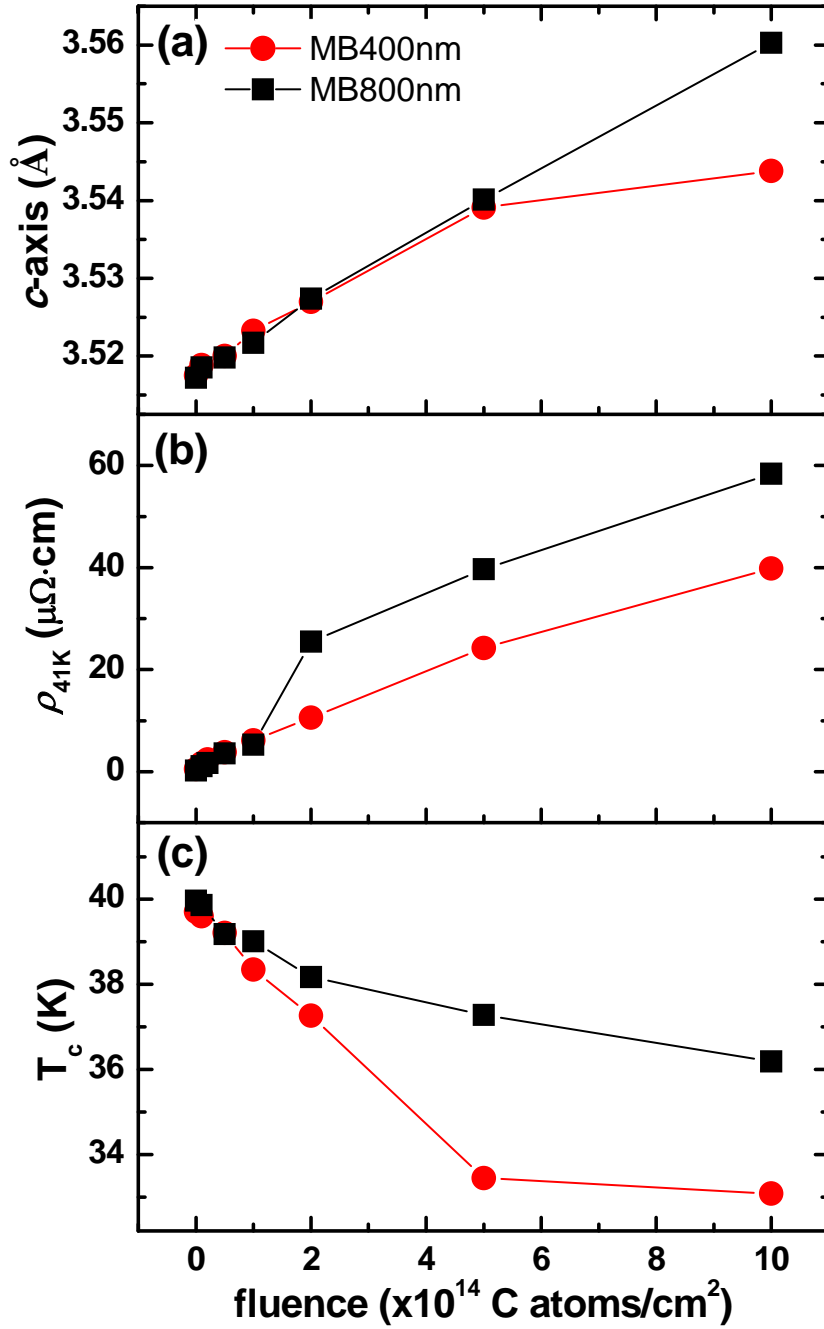


Figure 5. Fluence dependence of (a) c -axis lattice parameter, (b) residual resistivity (ρ_{41K}) and (c) T_c . T_c of MB400nm decreased more rapidly than that of MB800nm with increasing fluence, on the other hand, ρ_{41K} of MB800nm becomes much larger than that of MB400nm at the fluence of 2×10^{14} C atoms/cm 2 .

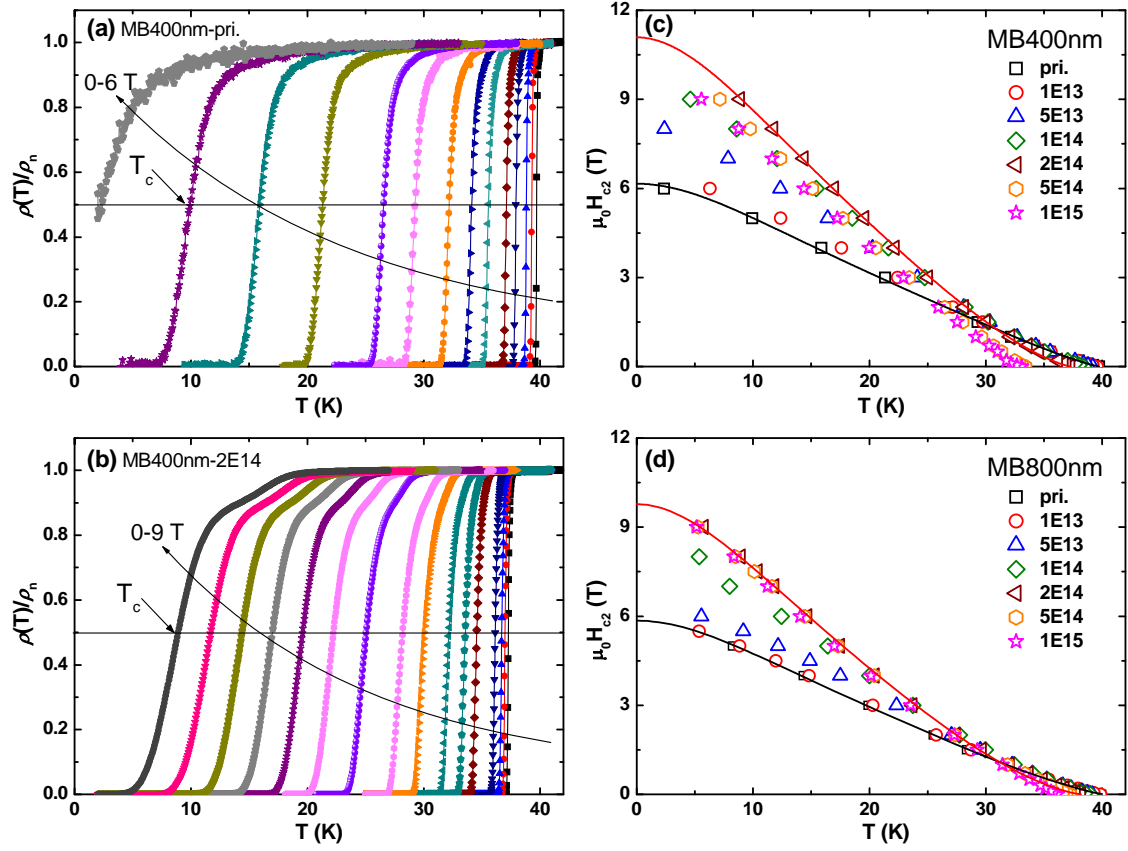


Figure 6. Temperature dependence of normalized resistivity, $\rho(T)/\rho_n$, for (a) pristine (pri.) and (b) 2×10^{14} C atoms/cm² (2E14) C-ion irradiated MB400nm in magnetic fields. Upper critical field ($\mu_0 H_{c2}$) as a function of temperature for (c) MB400nm and (d) MB800nm for various fluences. Solid lines in figures 6(c) and (d) represent fitting curves for the $H_{c2}(T)$ of the pristine and irradiated (2E14) MgB₂ films, obtained from two-band GL theory.

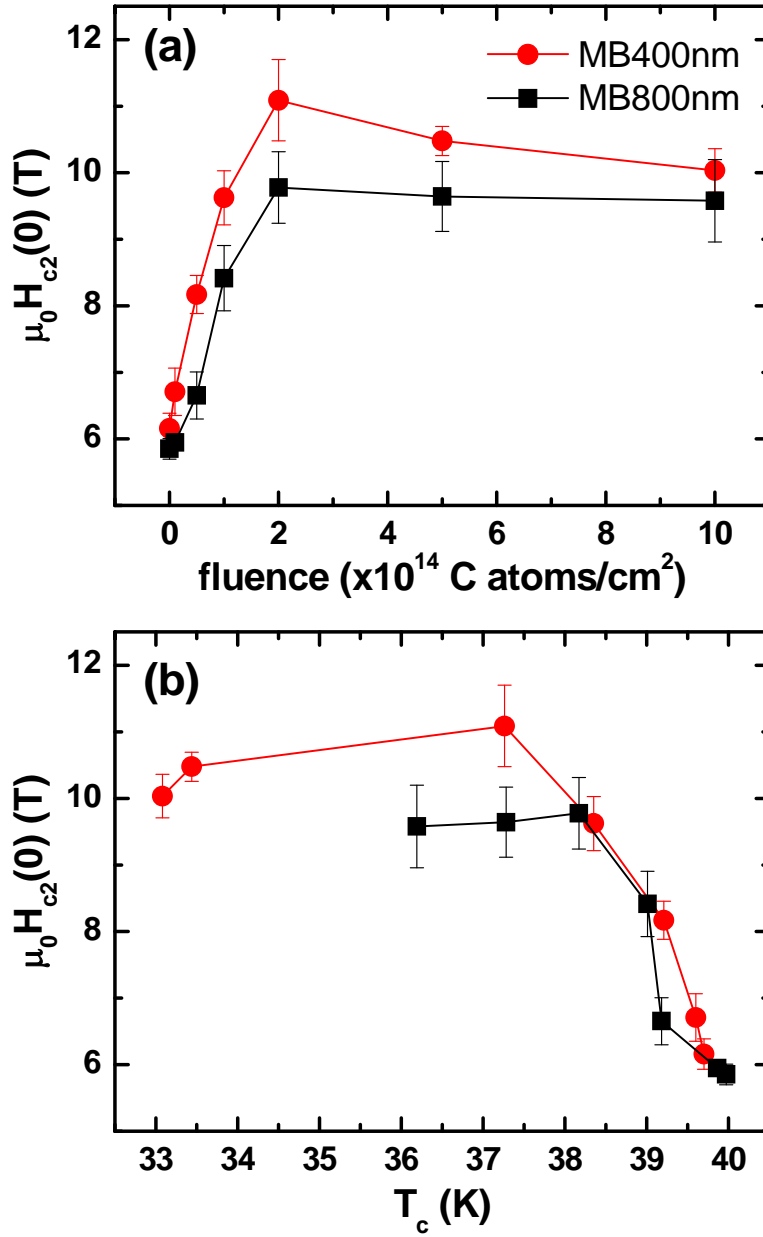


Figure 7. Zero-temperature upper critical fields, $\mu_0 H_{c2}(0)$, of MB400nm and MB800nm as functions of (a) fluence and (b) superconducting transition temperature (T_c). Both samples show the largest increase of $\mu_0 H_{c2}(0)$ at the fluence of 2×10^{14} C atoms/cm². The error bars on the $\mu_0 H_{c2}(0)$ reflect uncertainties in the measured $H_{c2}(T)$ s and fitting curves given by two-band GL theory.

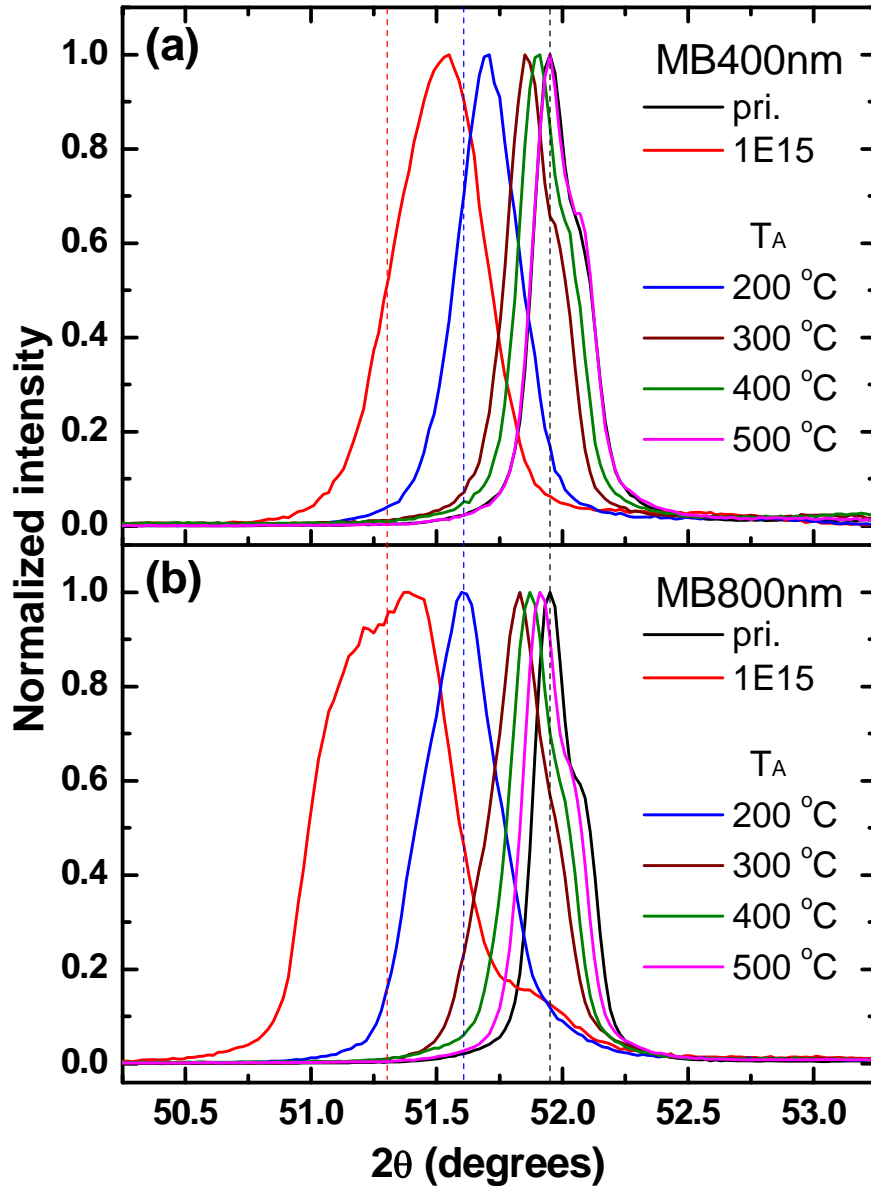


Figure 8. XRD of $\theta - 2\theta$ scans around (002) peak for (a) 1×10^{15} C atoms/cm² (1E15) irradiated MB400nm and (b) MB800nm after thermal annealing at various temperatures. The moved peak position due to irradiation is gradually restored to its position in the pristine state with increasing annealing temperature (T_A), and the (002) peak position of MB400nm fully restored after annealing at 500 °C. The dashed lines are guides for the eyes for comparison of MB400nm and MB800nm.

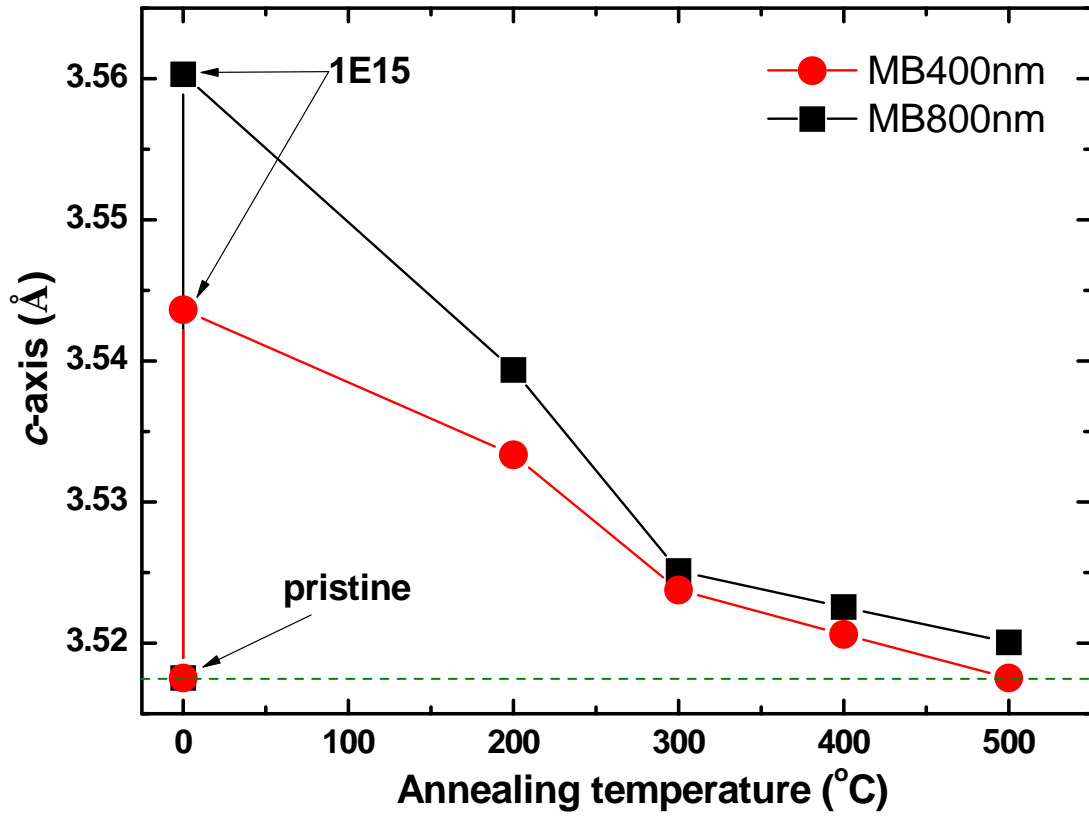


Figure 9. *c*-axis lattice parameter as a function of annealing temperature for 1×10^{15} C atoms/cm² (1E15) irradiated MB400nm and MB800nm, calculated from the (002) peak shown in figure 8. The dashed line is a guide for the eyes.

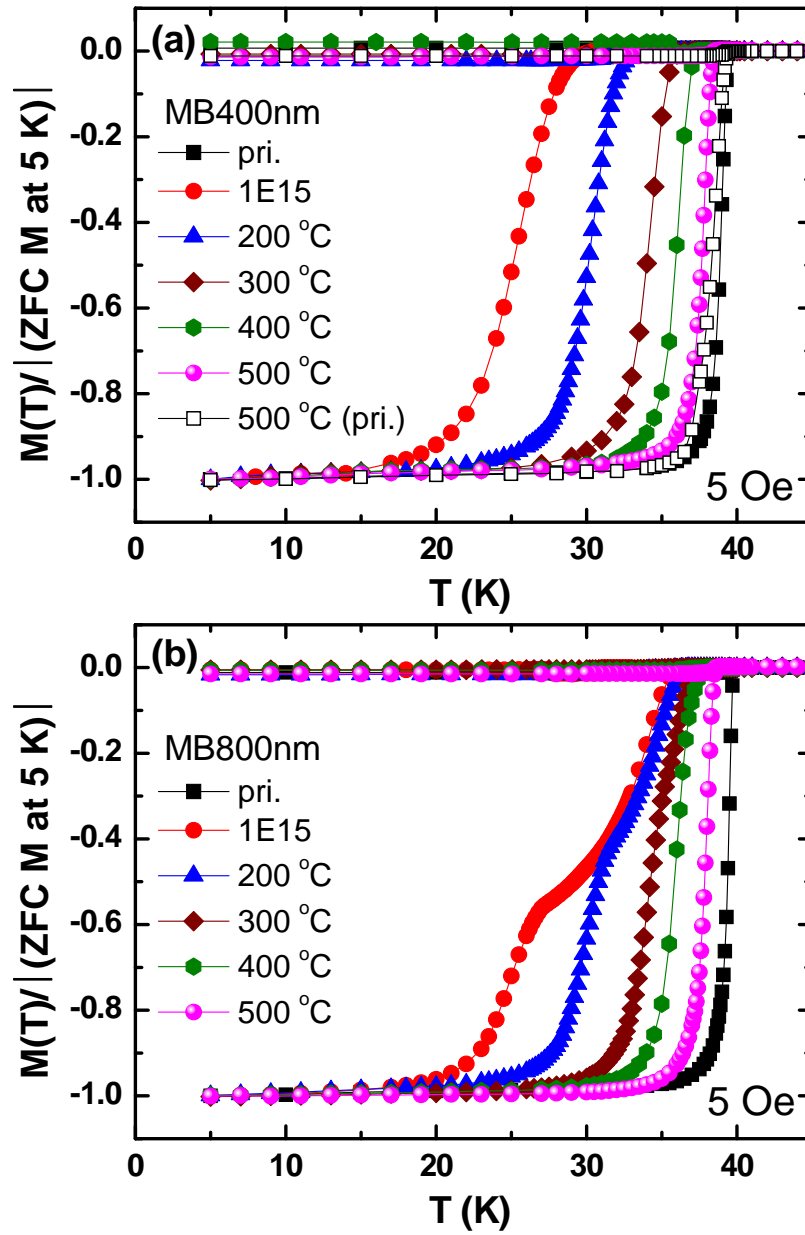


Figure 10. Temperature dependence of magnetization (M) for 1×10^{15} C atoms/cm² (1E15) irradiated (a) MB400nm and (b) MB800nm after thermal annealing at various temperatures. $M(T)$ values are normalized by each ZFC M value at 5 K for comparison. The superconductivity of both irradiated MB400nm and MB800nm films is almost restored to that in the pristine state after annealing at 500 °C.

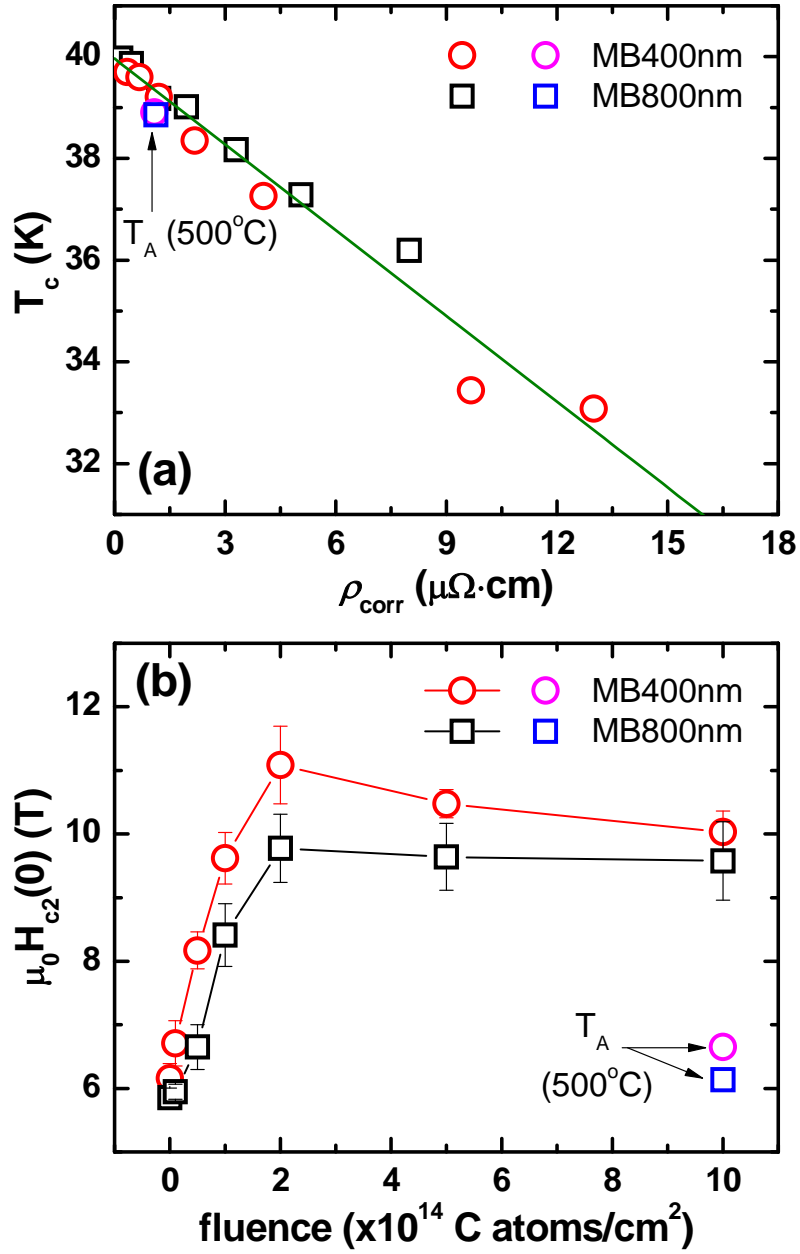


Figure 11. (a) T_c for irradiated MB400nm and MB800nm and sequentially annealed 1×10^{15} C atoms/cm² ($1E15$) irradiated films at $T_A = 500$ °C vs. corrected residual resistivity, ρ_{corr} . T_c variation after annealing is also well expressed by the function of ρ_{corr} . (b) Change in $\mu_0 H_{c2}(0)$ for irradiated MB400nm ($1E15$) and MB800nm ($1E15$) after annealing at $T_A = 500$ °C. $\mu_0 H_{c2}(0)$ values for both films after annealing largely decrease and are close to those for the pristine films.

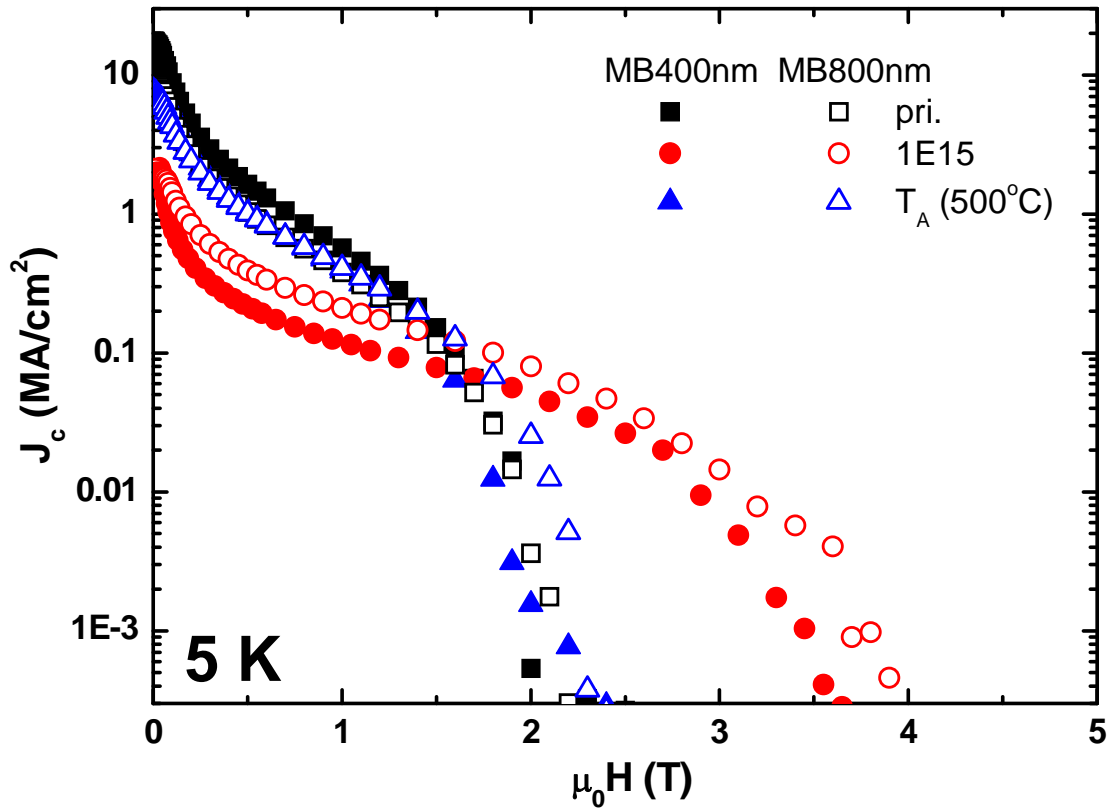


Figure 12. Critical current density (J_c) at 5 K as a function of magnetic field for MB400nm and MB800nm: pristine, 1×10^{15} C atoms/cm² (1E15) irradiated, and annealed at 500 °C. Field performance of J_c for irradiated films (1E15) became much stronger than that of pristine (pri.) samples despite a large suppression of low-field J_c . Interestingly, field dependence of J_c , $J_c(H)$, for both the irradiated films became comparable with $J_c(H)$ for pristine films after annealing them at $T_A = 500$ °C.

References

- [1] Nagamatsu J, Nakagawa N, Muranaka T, Zenitani Y and Akimitsu J 2001 Superconductivity at 39 K in magnesium diboride *Nature* **410** 63
- [2] Xi X X 2008 Two-band superconductor magnesium diboride *Rep. Prog. Phys.* **71** 116501
- [3] Gurevich A *et al* 2003 Very high upper critical fields in MgB₂ produced by selective tuning of impurity scattering *Supercond. Sci. Technol.* **17** 278
- [4] Larbalestier D C *et al* 2001 Strongly linked current flow in polycrystalline forms of the superconductor MgB₂ *Nature* **410** 186
- [5] Kim H- J, Kang W N, Choi E- M, Kim M- S, Kim K H P and Lee S- I 2001 High current-carrying capability in *c*-axis-oriented superconducting MgB₂ thin films *Phys. Rev. Lett.* **87** 087002
- [6] Choi H J, Roundy D, Sun H, Cohen M L and Louie S G 2002 The origin of the anomalous superconducting properties of MgB₂ *Nature* **418** 758
- [7] Souma S, Machida Y, Sato T, Takahashi T, Matsui H, Wang S- C, Ding H, Kaminski A, Campuzano J C, Sasaki S and Kadowaki K 2003 The origin of multiple superconducting gaps in MgB₂ *Nature* **423** 65
- [8] Wilke R H T, Bud'ko S L, Canfield P C, Finnemore D K, Suplinskas R J and Hannahs S T 2004 Systematic effects of carbon doping on the superconducting properties of Mg(B_{1-x}C_x)₂ *Phys. Rev. Lett.* **92** 217003
- [9] Dou S X, Yeoh W K, Horvat J and Ionescu M 2003 Effect of carbon nanotube doping on critical current density of MgB₂ superconductor *Appl. Phys. Lett.* **83** 4996.
- [10] Karpinski J, Zhigadlo N D, Katrych S, Puzniak R, Rogacki K and Gonnelli R 2007 Single

crystals of MgB₂: Synthesis, substitutions and properties *Physica C* **456** 3

[11] Li W X, Xu X, Chen Q H, Zhang Y, Zhou S H, Zeng R and Dou S X 2011 Graphene micro-substrate-induced π gap expansion in MgB₂ *Acta Mater.* **59** 7268

[12] Ferrando V *et al* 2007 Systematic study of disorder induced by neutron irradiation in MgB₂ thin films *J. Appl. Phys.* **101** 043903

[13] Putti M, Vaglio R and Rowell J M 2008 Radiation effects on MgB₂: a review and a comparison with A15 superconductors *Supercond. Sci. Technol.* **21** 043001

[14] Wilke R H T, Bud'ko S L, Canfield P C, Farmer J and Hannahs S T 2006 Systematic study of the superconducting and normal-state properties of neutron-irradiated MgB₂ *Phys. Rev. B.* **73** 134512

[15] Tarantini C *et al* 2006 Effects of neutron irradiation on polycrystalline Mg¹¹B₂ *Phys. Rev. B.* **73** 134518

[16] Bugoslavsky Y, Cohen L F, Perkins G K, Polichetti M, Tate T J, Gwilliam R and Caplin A D 2001 Enhancement of the high-magnetic-field critical current density of Superconducting MgB₂ by proton irradiation *Nature* **411** 561

[17] Gandikota R *et al* 2005 Effect of damage by 2 MeV He ions and annealing on H_{c2} in MgB₂ thin films *Appl. Phys. Lett.* **87** 072507

[18] Chikumoto N, Yamamoto A, Konczykowski M and Murakami M 2002 Magnetization behavior of MgB₂ and the effect of high energy heavy-ion irradiation *Physica C* **378** 466

[19] Shinde S R *et al* 2004 Modification of critical current density of MgB₂ films irradiated with 200 MeV Ag ions *Appl. Phys. Lett.* **84** 2352

[20] Civale L, Marwick A D, Worthington T K, Kirk M A, Thompson J R, Krusin-Elbaum L,

- Sun Y, Clem J R and Holtzberg F 1991 Vortex confinement by columnar defects in $\text{YBa}_2\text{Cu}_3\text{O}_7$ crystals: enhanced pinning at high fields and temperatures *Phys. Rev. Lett.* **67** 648
- [21] Yang P and Lieber C M 1996 Nanorod-superconductor composites: A pathway to materials with high critical current densities *Science* **273** 1836
- [22] Olsson R J, Kwok W- K, Karapetrov G, Iavarone M, Claus H, Peterson C and Crabtree G W 2002 Effect of high energy heavy ion irradiation on *c*-axis oriented MgB_2 films arXiv:cond-mat/0201022.
- [23] Parkin D M 1990 Radiation effects in high-temperature superconductors: A brief review *Metall. Trans. A* **21A** 1015
- [24] Fritzsche C 1978 Ion implantation into semiconductors *Angew. Chem. Int. Ed. Engl.* **17** 496
- [25] Klein K M, Park C and Tasch A F 1992 Monte Carlo simulation of boron implantation into single-crystal silicon *IEEE T. Electron. Dev.* **39** 1614
- [26] Eisterer M 2018 Radiation effects on iron-based Superconductors *Supercond. Sci. Technol.* **31** 013001
- [27] Matsushita T 2007 *Flux Pinning in Superconductors* (Springer, Berlin)
- [28] Seong W K, Oh S and Kang W N 2012 Perfect domain-lattice matching between MgB_2 and Al_2O_3 : single-crystal MgB_2 thin films grown on sapphire *Jpn. J. Appl. Phys.* **51** 083101
- [29] Seong W K, Huh J Y, Jung S- G, Kang W N, Lee H S, Choi E- M and Lee S- I 2007 Growth of superconducting MgB_2 thin films by using hybrid physical-chemical vapor deposition *J. Kor. Phys. Soc.* **51** 174
- [30] The mean projected range of C ions in the MgB_2 was calculated using the SRIM software. (www.srim.org/)

- [31] Huh J Y, Seong W K, Jung S -G and Kang W N 2007 Influence of Mg deficiency on superconductivity in MgB₂ thin films grown by HPCVD *Supercond. Sci. Technol.* **20** 1169
- [32] Rowell J M 2003 The widely variable resistivity of MgB₂ samples *Supercond. Sci. Technol.* **16** R17
- [33] Wang J, Zhuang C G, Li J, Wang Y Z, Feng Q R and Zheng D N 2009 Upper critical field and Raman spectra of MgB₂ thin films irradiated with low energy oxygen ion *J. App. Phys.* **106** 093915
- [34] Askerzade İ N, Gencer A and Güçlü N 2002 On the Ginzburg-Landau analysis of the upper critical field H_{c2} in MgB₂ *Supercond. Sci. Technol.* **15** L13
- [35] Chu M H, Martínez-Criado G, Segura-Ruiz J, Geburt S and Ronning C 2013 Local lattice distortions in single Co-implanted ZnO nanowires *Appl. Phys. Lett.* **103** 141911
- [36] Chu M H, Martínez-Criado G, Segura-Ruiz J, Geburt S and Ronning C 2014 Nano-X-ray diffraction study of single Co-implanted ZnO nanowires *Phys. Status Solidi A* **211** 2523
- [37] Jorgensen J D, Hinks D G and Short S 2001 Lattice properties of MgB₂ versus temperature and pressure *Phys. Rev. B.* **63** 224522
- [38] Pogrebnyakov A V *et al* 2004 Enhancement of the superconducting transition temperature of MgB₂ by a strain-induced bond-stretching mode softening *Phys. Rev. Lett.* **93** 147006
- [39] Cui Y, Po G and Ghoniem N 2017 Does irradiation enhance or inhibit strain bursts at the submicron scale? *Acta Mater.* **132** 285
- [40] Zehetmayer M, Eisterer M, Jun J, Kazakov S M, Karpinski J, Birajdar B, Eibl O and Weber H W 2004 Fishtail effect in neutron-irradiated superconducting MgB₂ single crystals *Phys. Rev. B.* **69** 054510